minerals

MDPI

Article

Sulfate and Freeze-Thaw Resistance of Porous Geopolymer Based on Waste Clay and Aluminum Salt Slag

Girts Bumanis [1,*], Diana Bajare [2], Aleksandrs Korjakins [2] and Danutė Vaičiukynienė [1]

[1] Faculty of Civil Engineering and Architecture, Kaunas University of Technology, Studentu St. 48, LT-51367 Kaunas, Lithuania
[2] Department of Building Materials and Products, Faculty of Civil Engineering, Riga Technical University, Kipsalas iela 6A, LV-1048 Riga, Latvia
* Correspondence: girts.bumanis@rtu.lv; Tel.: +370-657-66-815

Abstract: The search for efficient waste source precursors for geopolymer production is active in scientific society. The feasibility of using calcined kaolin clay and fly ash as suitable precursors for the production of geopolymers is widely described and acknowledged. The availability and energy input required to produce such precursors hinders their competing with traditional binders, however. Therefore, new by-product source precursors are sought in different industries. In this research, three industrial origin secondary raw materials are examined as precursors for the production of porous geopolymers. Calcined illite or kaolin clay in combination with salt cake from the aluminium scrap recycling industry after alkali activation gives lightweight material from 540–675 kg/m^3. A comparison of the two precursors was made, and the physical and mechanical properties were determined. Freeze-thaw resistance and sulfate attack were used to characterize durability. Results indicate the role of waste clay type and salt cake content on geopolymer properties as materials with similar appearance performed differently. The results show that metakaolin based geopolymers outperformed red clay based geopolymers and they can withstand from 25 to 50 freeze-thaw cycles with strength loss from 10 to 65%. Sulfate attack showed significant strength loss for red clay based geopolymers after 61 days of soaking time in contrast to metakaolin based geopolymers.

Keywords: geopolymer; metakaolin; waste clay; porous material; sulfate resistance; freeze-thaw

Citation: Bumanis, G.; Bajare, D.; Korjakins, A.; Vaičiukynienė, D. Sulfate and Freeze-Thaw Resistance of Porous Geopolymer Based on Waste Clay and Aluminum Salt Slag. *Minerals* **2022**, *12*, 1140. https://doi.org/10.3390/min12091140

Academic Editor: Thomas N. Kerestedjian

Received: 2 August 2022
Accepted: 2 September 2022
Published: 8 September 2022

1. Introduction

Intensive research on geopolymer precursors and derived material properties has been performed in recent times. Many authors have found that alkali-activated pure metakaolin and fly ash produced cementitious material with good durability and mechanical properties [1–3]. However, the use of such precursors is expensive, and earth resources are depleting [3,4]. The potential of other silica and alumina-rich precursors, especially waste originated, has been widely researched lately [5–7]. One of such materials is demolished waste ceramic bricks. Waste brick is a widely available material, while up to now, it is usually used as low value aggregate and filling material after processing through rough crushing. Regarding waste particle size and reactivity, activator type, alkali dosage, and curing temperature, waste bricks are generally suitable for alkali activation [8,9]. Depending on the composition and activation solution, a material with strength from 7 to 58 MPa can be achieved [10,11]. Results have opened the possibility of partially or entirely replacing ordinary Portland cement in civil engineering.

Along with the energy efficiency of material production and the improved mechanical properties, the durability aspect has still been an argument to stick to the more conservative building materials [12]. Therefore, research on the durability of geopolymers is still an uncovered field to work on [13]. Lately, the use of recycled or waste materials as a precursor to develop high value-added geopolymers has been extended to enhance the freeze-thaw

resistance of civil engineering in the changing Nordic climate. The geopolymer concrete strength loss after 50 freeze-thaw cycles was reported between 6.11 and 66.85%, which was associated with the reduction of pH at very low temperatures [14]. It was concluded that the sodium silicate-activated geopolymers have higher freeze-thaw resistance than the NaOH-activated paste. Metakaolin and ground granulated blast-furnace slag geopolymer had compressive strength loss of samples ranging from 12 to 17% after 25 cycles. At the same time, the most concern was dedicated to coupling cycles, such as shrinkage induced by drying and wetting cycles, and the volume expansion caused by temperature fluctuation [15]. To replace concrete with geopolymer material in structural engineering, sulfate attack must be considered as groundwaters may often contain an aggressive environment. The slag/fly ash ratios affect the silicate modulus, which impacts the geopolymer sulfate resistance [16]. Ettringite and gypsum were the main degradation products [16,17], while extremely high strength loss was identified in the slag binders exposed to the $MgSO_4$ (60.53%–73.4%) as compared to the Na_2SO_4 solutions (7.2%–27.9%) after 84 days [17].

Salt slag, sometimes referred to as a salt cake, is the main waste generated from secondary aluminum production, which contains a mixture of aluminum and metal oxides and slag [18]. Salt slag contains 5–7 wt.% residual aluminum metal, 15–30 wt.% aluminum oxide, 30–55 wt.% sodium chloride, and 15–30 wt.% potassium chloride. Other impurities such as carbides, nitrides, phosphides, and sulfides might be are also present at different rates [19]. Highly toxic and poisonous gases such as NH_3, H_2S, PH_3, and CH_4 are formed when the salt cake interacts with water [20,21]. It is assumed that salt slags from the aluminum scrap recycling industry need to be recycled/treated as they are considered hazardous by-products. Previously, there were efforts to produce porous geopolymers using salt slag for water treatment of anaerobic digestion [22,23]. Porous geopolymers have been developed before for use in civil engineering, including such directions as insulation materials, heavy metal, and other pollutant absorbers [24–26].

This study investigates the performance of two different waste clay and salt slag precursor porous geopolymers' performance exposed to freeze-thaw cycles and sulfate attacks. Gas released from salt slag was entrapped in a geopolymer matrix, and a porous material structure was formed. The physical and mechanical properties of the obtained geopolymer were characterized.

2. Materials and Methods

2.1. Raw Materials

Two calcined clay precursors were used to prepare porous geopolymers. The first clay precursor originated from a ceramic brick production plant, and it is based on low-carbonate illite clay (IC). Red IC is used to produce construction brick, while part of damaged products is ground to sand particles (<2 mm) and used as an inert filler in further production. During the burning of bricks, the IC overgoes thermal treatment of around 1050 °C. After grinding, the specific surface area of ground IC was 1448 cm^2/g. Calcined IC has little crystalline structure and besides quartz (SiO_2) and illite ($K(AlFe)_2AlSiO_3O_{10}(OH)_2 \cdot H_2O$) it also contains microcline ($KAlSiO_8$). The chemical composition of calcined IC is given in Table 1.

Metakaolin (MK) precursor was obtained from an expanded glass granule production plant in Lithuania. In the final stage of a glass granule production process, kaolin clay is used for anti-agglutination. During the granule production, kaolin is subjected to 850 °C for about 40–50 min and metakaolin mineral is formed. In this research a MK fraction <0.25 mm was used for further experiments.

Salt slag (SL) from the aluminum scrap recycling factory was used as Al_2O_3 source and blowing agent to obtain porous geopolymers. IC and SL were ground in the laboratory planetary ball mill Retsch PM 400 for 30 min with a speed 300 rpm to obtain powder particles. All remaining metallic elements from SL were removed by sieving milled powder through 0.2 mm sieve. SL's chemical and mineralogical composition and other properties are provided in the previously published papers [27,28]. The SL contains metallic aluminum

(Al), iron sulfite ($FeSO_3$), aluminum nitride (AlN), corundum (Al_2O_3), aluminum iron oxide ($FeAlO_3$), magnesium dialuminium ($MgAl_2O_4$), quartz (SiO_2), aluminum chloride ($AlCl_3$) and aluminum hydroxide ($Al(OH)_3$). The chemical composition of SL is given in Table 1.

Table 1. Chemical composition of raw materials: SL, IC, MK, Q and D (wt.%).

Chemical Component	SL	IC	MK	Q	D
Al_2O_3	63.19	14.60	51.7	1.42	-
SiO_2	7.92	73.84	34.4	96.8	-
CaO	2.57	0.91	0.09	-	-
SO_3	0.36	-	-	-	-
TiO_2	0.53	0.63	0.55	-	-
MgO	4.43	1.10	0.13	-	-
Fe_2O_3	4.54	4.08	0.53	0.34	-
Na_2O	3.84	0.06	0.63	-	-
K_2O	3.81	2.75	0.01	-	-
$CaCO_3$*$MgCO_3$	-	-	-	-	97.0
Other	2.60	1.05	1.96	0.49	-
LOI, 1000 °C	6.21	0.98	10.1	0.95	3.0

Quartz (Q) and dolomite (D) filler with a maximum particle size of 0.3 mm was used as filler in the compositions. Alkali activators were prepared by using commercially available sodium silicate solution characterized by the silica modulus Ms 3.22. To obtain modified alkali activation solution with the required chemical composition, the addition of sodium hydroxide flakes was done to achieve sodium silicate solution with silica modulus of Ms 1.67. Commercially available sodium hydroxide flakes with 97% purity were used.

2.2. Mixture Composition

Four series of geopolymers with different SL content were prepared to obtain porous geopolymer (Table 2). SL content regarding clay was 10%, 50%, and 100%. Both clay and SL, together with an alkali activator, formed geopolymer paste, and the sodium silicate to clay and SL ratio was 0.75 for all mixtures. The D or Q sand was added as a filler with clay and SL to sand filler ratio of 1.0. At first, all dry components were mixed together, and then the alkali activator was incorporated into the mixture and mixed for 1 min. The prepared paste was immediately poured into a metal mold covered with plastic film before the blowing of paste occurred. Molds were covered with plastic film, and the cover and blowing of paste were followed. Then the samples were cured at 80 °C for 24 h. The density of porous AAM can be controlled by the amount of SL incorporated in the mixture design. The mixture amount in the mold was adjusted so that a complete specimen with a dimension of 40 × 40 × 160 mm was prepared. After cooling and demolding, samples were cured in a room environment until the testing day.

2.3. Test Methods

The chemical composition was determined for raw materials according to LVS EN-196-2 with sensibility ±0.5 wt.%, but elements were analyzed with EDX (energy dispersive X-ray spectrometry—EDS, Oxford instruments 7378). The particle size distribution for powdered raw material was determined by laser granulometer Analysette 22 Nano Tec. BET method (QuadraSorb) was used to determine surface area of powdered raw materials and porosity of AAM before and after a leaching test. Scanning electron microscope (SEM) (Tescan Mira/LMU) was used for microstructural investigation of AAM and for description of raw materials. The mineralogical composition by X-ray diffraction (XRD) (PAN analytical X'Pert PRO) was determined for raw materials and AAM.

The mechanical properties of geopolymers were tested according to LVS EN 1015-11 using specimens with dimensions 40 × 40 × 160 mm. Bulk density and water absorption were determined according to EN 1097-7 and EN 1097-6. Water saturated samples (72 h)

were used to calculate geopolymers' open porosity. Total porosity was calculated from specific gravity which was determined using a Le Chatelier flask (ASTM C188).

Table 2. Mixture composition of porous geopolymers based on IC and MK precursors.

Composition	IC	MK	SL	D	Q	Sodium Silicate Solution/Solid Ratio	Main Oxide Ratios	
							SiO_2/Al_2O_3	Na_2O/Al_2O_3
IC-0.1SL-Q	1.0	-	0.1	-	1.0	0.75	4.5	0.8
IC-0.5SL-Q	1.0	-	0.5	-	1.0	0.75	2.3	0.5
IC-1.0SL-Q	1.0	-	1.0	-	1.0	0.75	1.5	0.4
IC-0.1SL-D	1.0	-	0.1	1.0	-	0.75	4.5	0.8
IC-0.5SL-D	1.0	-	0.5	1.0	-	0.75	2.3	0.5
IC-1.0SL-D	1.0	-	1.0	1.0	-	0.75	1.5	0.4
MK-0.1SL-Q	-	1.0	0.1	-	1.0	0.75	2.4	0.4
MK-0.5SL-Q	-	1.0	0.5	-	1.0	0.75	1.6	0.4
MK-1.0SL-Q	-	1.0	1.0	-	1.0	0.75	1.1	0.3
MK-0.1SL-D	-	1.0	0.1	1.0	-	0.75	2.4	0.4
MK-0.5SL-D	-	1.0	0.5	1.0	-	0.75	1.6	0.4
MK-1.0SL-D	-	1.0	1.0	1.0	-	0.75	1.1	0.3

The thermal conductivity was measured with heat flow meter instrument LaserComp FOX 660 using air-dry geopolymer samples with dimensions 300 × 300 × 50 mm.

The freeze-thaw resistance of porous geopolymer samples were conducted according to the National annex of Latvian standard to European standard EN 206-1—Part 1: Requirements for classification and attestation of conformity LVS 156-1:2009 [29]. Six prismatic geopolymer samples with dimensions of 40 × 40 × 160 mm were water saturated for 72 h and then subjected to a freeze cycle at −18 °C. After 12 h, samples were defrosted in water before the next freezing cycle. Mass loss and strength loss were detected after 25 or 50 freeze-thaw cycles.

Sulfate resistance of porous geopolymers was determined according to SIA 262/1—Appendix D: Sulfate resistance [30]. The mass changes were recorded for geopolymer specimens with dimensions of 40 × 40 × 160 mm.

3. Results

3.1. Macrostructure

The macrostructure of the obtained geopolymer samples is given in Figure 1. The porous structure for all specimens is clearly visible. Heterogenous pore structure with uneven and chaotically formed pores was obtained for geopolymers based on IC. Macro pore size was in a range from 0.5 to 8 mm. A higher amount of SL revealed a more advanced pore structure. The geopolymer color was affected by the SL content; the less SL was in the mixture, the more intense was the color, being closer to the natural color of the clay precursor. The pore structure for geopolymers based on MK was more homogeneous for mixture compositions with SL content of 0.5 and 1.0. Macro pore size from 0.5 to 2 mm was predominant. The porous structure for sample MK-0.1SL-Q was similar to that of the IC clay precursor geopolymer.

3.2. Microstructure

The microstructure of the geopolymer pore wall cross section is given in Figure 2. It is clearly visible that besides macro pores, micropores from 10–50 μm are formed for geopolymers based on IC. A smooth pore surface can be observed with some crystal-shaped elements in their volume. Similar observations can be identified for geopolymer based on MK. A more refined pore structure (1–10 μm) was detected, and crystal compounds were formed between pore walls.

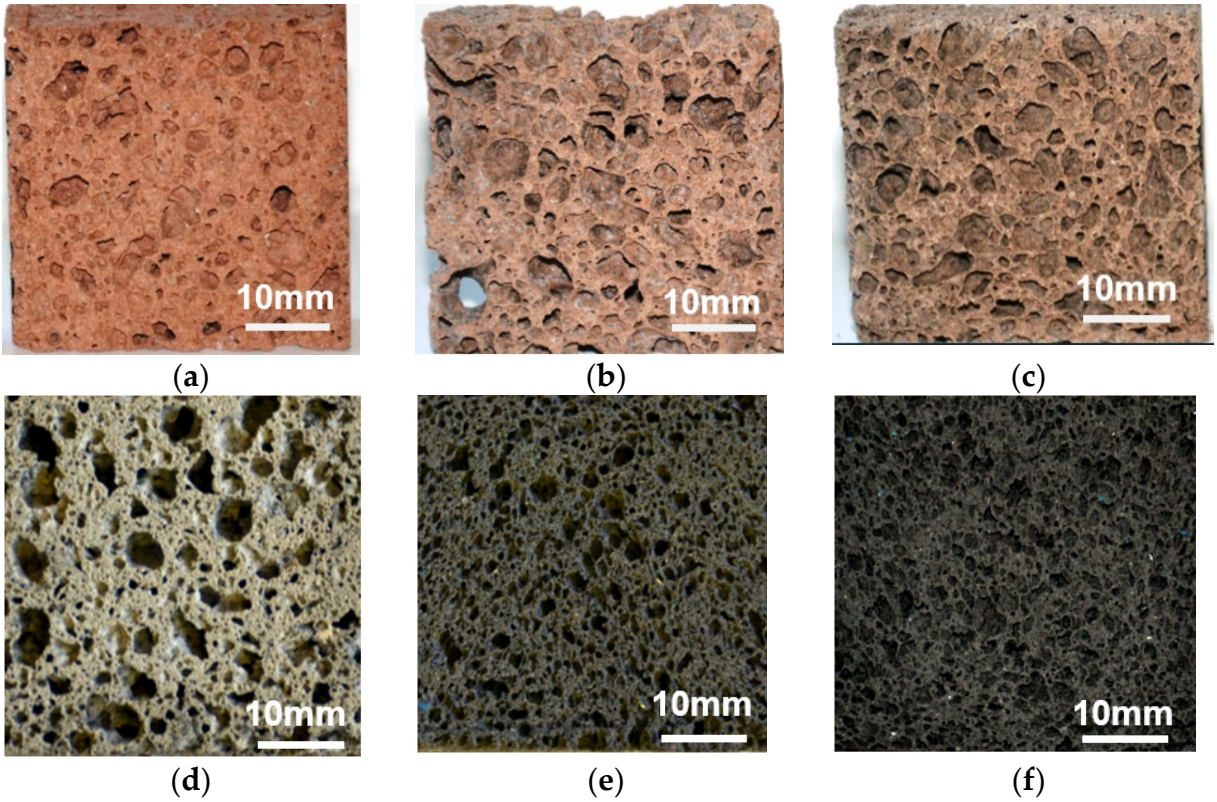

Figure 1. Macrostructure of porous geopolymers: (**a**) IC-0.1SL-Q, (**b**) IC-0.5SL-Q, (**c**) IC-1.0SL-Q, (**d**) MK-0.1SL-Q, (**e**) MK-0.5SL-Q, (**f**) MK-1.0SL-Q.

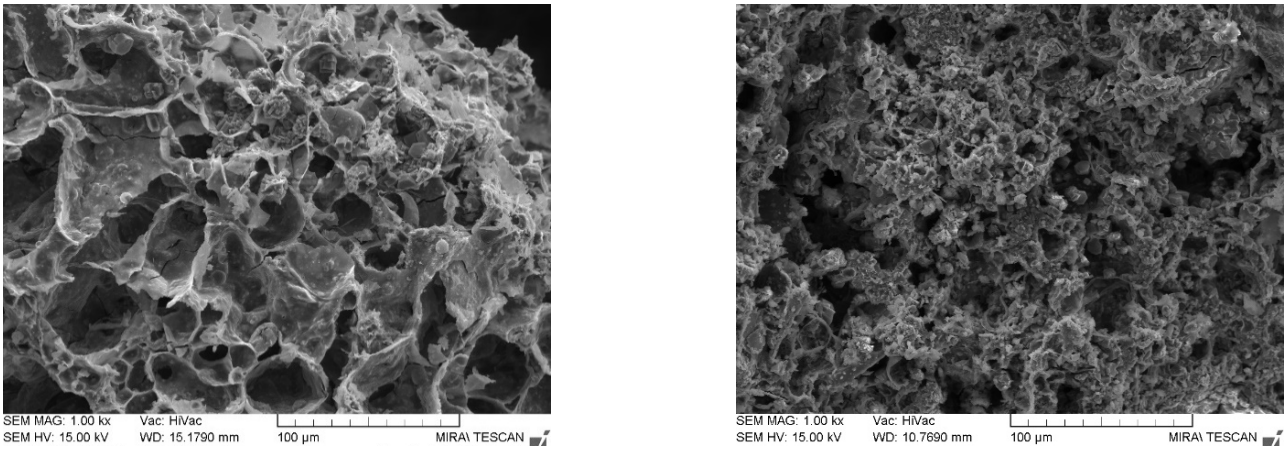

Figure 2. Microstructure of porous geopolymers: (**a**) IC-1SL-Q, (**b**) MK-1SL-Q.

3.3. Mineralogical Composition

The mineralogical composition of precursors and geopolymers without filler material is given in Figure 3. For IC precursor, mullite, montmorillonite, muscovite and microcline can be identified. For MK, kaolin mineral and quartz were identified. SL mineralogical composition contained iron sulfite ($FeSO_3$), magnesium dialuminium ($MgAl_2O_4$), aluminum nitride (AlN), aluminum iron oxide ($FeAlO_3$), quartz (SiO_2), aluminum chloride ($AlCl_3$) aluminum hydroxide ($Al(OH)_3$) and metallic aluminum (Al). After alkali activation, no crystalline phases were detected except for quartz.

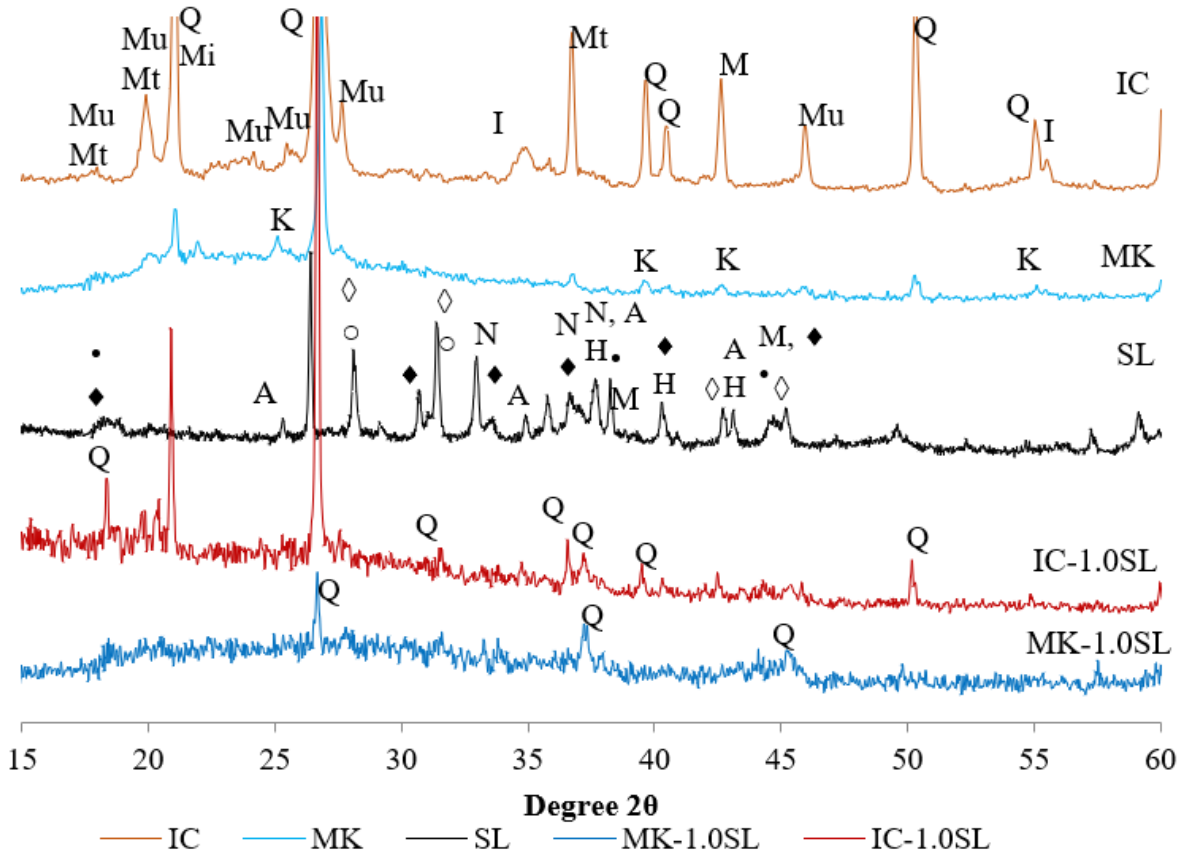

Figure 3. Mineralogical composition of raw precursors and geopolymers without fillers. ♦—$FeAlO_3$, •—$MgAl_2O_4$, A—Al_2O_3, Q-SiO_2, ◊—Fe_2SO_3, ○—$AlCl_3$, N—AlN, H—$Al(OH)_3$, M—metallic aluminium, Mu—muscovite, Mt—montmorillonite, I—illite, K—kaolin, Q—quartz.

3.4. Physical and Mechanical Properties

The physical and mechanical properties of porous geopolymers are given in Table 3. A small proportion of SL (0.1) in the mixture composition gives a highly porous geopolymer with a density of 655 to 675 kg/m^3. Increased amounts of SL (0.5 and 1.0) changed the bulk density from 555 to 620 kg/m^3. The lower density was for geopolymers based on IC (555 and 585 kg/m^3), while for mixtures with MK, the density was from 620 to 620 kg/m^3. The open porosity for geopolymers based on IC was similar for all mixtures from 29.4 to 33.4 vol.% and for MK—from 21.2 to 33.4 vol.%. The total porosity was from 72.0 to 78.4 vol.%, which describes a relation between porosity and density of the porous geopolymer. The water absorption was high due to high open porosity, from 41.5 to 54.4 wt.% for geopolymers based on IC and from 31.7 to 56.3 wt.% for mixtures with MK.

The mechanical properties are given in Table 3. Geopolymers based on IC, in general, had lower compressive strength compared to those based on MK. The compressive strength of IC based geopolymers was from 1.4 to 2.0 MPa and was little affected by its density. The flexural strength was 0.6 MPa for geopolymers with higher SL content and increased to 1.0 MPa with lower SL content. The strength decreased with the increase of porosity. MK-based geopolymers had compressive strength of 2.0 MPa for samples with higher porosity, and it increased to 3.8 MPa for samples with lower SL content. Flexural strength reduced similarly as for IC precursor samples, from 2.1 MPa for compositions with 0.1 SL to 1.4 MPa for compositions with 1.0 SL. The similar tendencies as for IC were observed here.

Table 3. Physical and mechanical properties of porous geopolymers.

Mixture Composition	Bulk Density, kg/m^3	Water Absorption, W_t,%	Open Porosity, vol.%	Total Porosity, vol.%	Compressive Strength, f_c, MPa	Bending Strength, f_m, MPa
IC-0.1SL-Q	655 ± 16	41.5 ± 2.5	33.4 ± 0.8	73.6 ± 1.2	1.9 ± 0.1	1.0 ± 0.08
IC-0.5SL-Q	585 ± 12	49.0 ± 3.7	31.0 ± 2.8	76.8 ± 1.5	1.5 ± 0.1	0.7 ± 0.03
IC-1.0SL-Q	540 ± 27	52.8 ± 2.7	29.7 ± 1.6	78.6 ± 1.8	1.7 ± 0.1	0.6 ± 0.05
IC-0.1SL-D	675 ± 17	41.5 ± 1.7	30.3 ± 1.3	73.0 ± 1.3	2.0 ± 0.1	0.9 ± 0.02
IC-0.5SL-D	555 ± 16	55.2 ± 3.2	33.0 ± 0.7	78.0 ± 2.0	1.4 ± 0.1	0.6 ± 0.03
IC-1.0SL-D	550 ± 16	54.4 ± 4.7	29.4 ± 0.8	78.4 ± 1.5	1.7 ± 0.1	0.6 ± 0.02
MK-0.1SL-Q	675 ± 13	31.9 ± 2.3	21.7 ± 1.2	71.4 ± 0.5	3.8 ± 0.2	2.1 ± 0.16
MK-0.5SL-Q	610 ± 13	41.1 ± 2.1	25.0 ± 1.1	74.9 ± 0.5	3.1 ± 0.2	1.7 ± 0.06
MK-1.0SL-Q	600 ± 14	52.5 ± 2.8	30.7 ± 2.1	75.9 ± 0.6	2.0 ± 0.1	1.4 ± 0.14
MK-0.1SL-D	670 ± 12	31.7 ± 1.2	21.2 ± 0.6	72.0 ± 0.5	3.8 ± 0.3	2.1 ± 0.11
MK-0.5SL-D	620 ± 14	47.3 ± 1.9	29.5 ± 1.0	74.5 ± 0.6	3.1 ± 0.2	1.5 ± 0.13
MK-1.0SL-D	580 ± 10	56.3 ± 2.9	33.4 ± 2.4	76.0 ± 1.0	2.4 ± 0.2	1.4 ± 0.07

3.5. Freeze-Thaw Resistance

The freeze-thaw resistance of porous geopolymers is given in Table 4. Results after 25 freeze-thaw cycles of fully saturated geopolymers indicate the structural changes which led to a strength decrease. MK based geopolymers had slight weight loss due to freezing and thawing after 25 freeze-thaw cycles. The weight loss was 3.3 for MK with high SL content and it increased to 6.5% for samples with low SL content. The highest weight loss was for the mixture with quartz filler. There was a different performance during the first 25 freeze-thaw cycles for geopolymers based on IC. Significant weight loss was detected, and it ranged from 6.9 to 14.4%. As a result, visible destruction of samples was detected for all specimens. Geopolymers based on MK were further subjected up to 50 freeze-thaw cycles. Weight change was 6.6% for composition with 0.5 SL and increased to 15.5% for 0.1 SL with Q filler, which was still less than IC counterparts after 25 cycles. The highest weight loss was for geopolymer with low SL content and Q filler. Strength loss increased significantly as reduction reached from 22.6 to 65.8%. The highest strength reduction was for the mixture with the lowest SL content, and also composition MK-1.0SL-D showed high strength reduction.

Table 4. Freeze-thaw resistance of porous geopolymers based on IC and MK.

Composition	Δm, %		Initial Strength, MPa	Residual Strength, MPa		Strength Change, %	
	No. of Cycles			No. of Cycles		No. of Cycles	
	25	50		25	50	25	50
IC-0.1SL-Q	−8.0	-	1.9 ± 0.1	1.2 ± 0.2	-	36.8	-
IC-0.5SL-Q	−6.9	-	1.5 ± 0.1	1.3 ± 0.2	-	13.3	-
IC-1.0SL-Q	−14.4	-	1.7 ± 0.1	1.1 ± 0.2	-	35.3	-
IC-0.1SL-D	−9.3	-	2.0 ± 0.1	1.1 ± 0.1	-	45.0	-
IC-0.5SL-D	−9.7	-	1.4 ± 0.1	1.0 ± 0.2	-	28.6	-
IC-1.0SL-D	−11.6	-	1.7 ± 0.1	1.1 ± 0.2	-	35.3	-
MK-0.1SL-Q	−6.5	−15.5	3.8 ± 0.2	1.7 ± 0.2	1.3 ± 0.1	55.3	65.8
MK-0.5SL-Q	−3.5	−6.2	3.1 ± 0.2	2.4 ± 0.2	2.2 ± 0.4	22.6	29.0
MK-1.0SL-Q	−3.3	−8.4	2.0 ± 0.1	1.8 ± 0.2	1.5 ± 0.2	10.0	25.0
MK-0.1SL-D	−3.6	−8.8	3.8 ± 0.3	2.6 ± 0.3	1.9 ± 0.2	31.6	50.0
MK-0.5SL-D	−3.7	−6.6	3.1 ± 0.2	2.6 ± 0.2	2.4 ± 0.3	16.1	22.6
MK-1.0SL-D	−3.6	−9.9	2.4 ± 0.2	2.0 ± 0.1	1.1 ± 0.1	16.7	54.2

3.6. Sulfate Attack

The weight and strength change of geopolymer samples subjected to sulfate solution for 61 days is given in Table 5. The final weight of the samples showed different results for

geopolymers based on IC. Some of the samples lost weight, while for some compositions, the weight increased. For MK samples, the final weight changes increased. The dynamic weight change during the test is given in Figure 4. It can be seen that some of the samples at the beginning had gradual weight loss and then weight increase again, while the others had weight increase and then small fluctuation might occur.

Table 5. Sulfate attack test results.

Mixture	Weight Change, %	Initial Compressive Strength, MPa	Residual Compressive Strength, Mpa	Compressive Strength Change, %
IC-0.1SL-Q	−5.5	1.9 ± 0.1	0.8 ± 0.1	−57.9
IC-0.5SL-Q	0.9	1.5 ± 0.1	1.0 ± 0.1	−33.3
IC-1.0SL-Q	−1.6	1.7 ± 0.1	1.1 ± 0.1	−35.3
IC-0.1SL-D	2.9	2.0 ± 0.1	1.8 ± 0.4	−10.0
IC-0.5SL-D	0.61	1.4 ± 0.1	1.1 ± 0.2	−21.4
IC-1.0SL-D	−9.3	1.7 ± 0.1	1.2 ± 0.1	−29.4
MK-0.1SL-Q	2.1	3.8 ± 0.2	2.1 ± 0.2	−44.7
MK-0.5SL-Q	4.2	3.1 ± 0.2	2.6 ± 0.2	−16.1
MK-1.0SL-Q	2.2	2.0 ± 0.1	1.9 ± 0.3	−5.0
MK-0.1SL-D	1.2	3.8 ± 0.3	2.8 ± 0.3	−26.3
MK-0.5SL-D	0.1	3.1 ± 0.2	2.7 ± 0.3	−12.9
MK-1.0SL-D	0.2	2.4 ± 0.2	2.4 ± 0.2	0.0

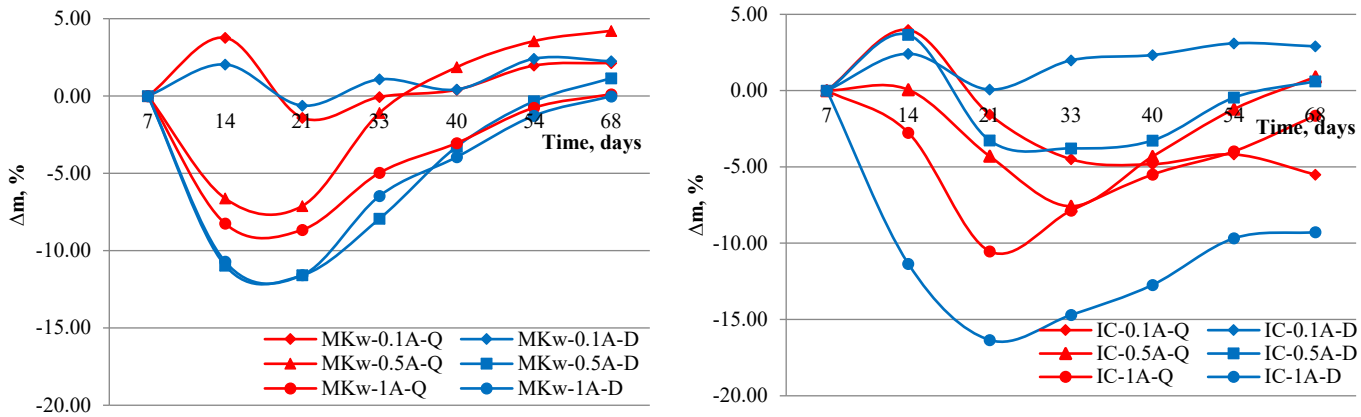

(**a**) (**b**)

Figure 4. Weight change during sulfate attack test: (**a**) MK based geopolymers, (**b**) IC based geopolymers.

The strength reduction after sulfate attack was from 10 to 57.9% for compositions with IC and from 0 to 44.7% for compositions based on MK. Higher strength loss was for samples with low SL content. For denser samples with higher initial strength, the sulfate attack did more damage to the structure than for more porous materials. IC showed higher strength loss than its MK counterparts. MK based geopolymers with high SL content showed strength loss from 0.0 to 5.0%.

4. Discussion

The structural difference between the samples is determined mainly by the content of SL. The amount of gas-releasing agent SL significantly influenced the geopolymer's porosity. For all geopolymers based on IC, the pore structure was similar, while the volume of pores was different. The higher was the amount of SL in the composition, the more pronounced pore structure was formed. Density and water absorption results confirmed this. A reduced amount of SL (0.1) made larger pores, and the structure is more similar to that of geopolymers based on IC. This could be associated with the fineness of the precursor (MK), as it has a finer particle size than IC. More stable paste and gas released

from SL can be entrapped easier in smaller bubbles. At the same time, for geopolymers made with an IC precursor, the coarser nature of IC results in pore coalescence. Such pores allow water media to infiltrate into deeper layers on the material much faster and could thus affect the durability of the geopolymers. Pore size distribution can affect both freeze-thaw resistance and other chemical attack penetration in geopolymers and lead to its structural deterioration or change. Pore structure can affect thermal performance of geopolymers as previously it was determined that density decrease to 950 kg/m^3 can improve thermal conductivity to 0.33 W/mK [31]. The other factor affecting pore structure formation is associated with the endothermic reaction, which occurs during gas release from SL. Previously it was reported that during gas release, the temperature of the geopolymer paste, depending on SL content, could increase up to 98 °C [32]. Lower SL content resulted in lower heat increase and slower stabilization of pore wall structure of the geopolymers.

In contrast, the rapid temperature increase for high SL content material instantly sets the geopolymer paste and stabilizes a finer pore structure. Nucleation of gas bubbles inside the geopolymer matrix suppresses the bubbles' growth as the temperature increase hardens the structure of the geopolymers. Lower temperature increase or coarser structure of geopolymer precursors allow the growth and coalescence of the pores.

For both precursors (IC and MK) the bulk density was similar, and little influence of selected filler was observed. The lowest density was for geopolymers with the highest SL content—from 540 to 600 kg/m^3. The density reduction was not observed, which could be associated with the heat increase during the geopolymer structure's gas release and stabilization time. This phenomenon should be investigated more deeply in further research. For geopolymers based on MK, the influence of SL content on open porosity was more expressed by the results. High open porosity could be associated with gas release and remaining capillary porosity as is traditional for coarse ceramic materials, e.g., bricks [33]. Lower water absorption was found for geopolymers with a higher density as open porosity determines water uptake for the samples.

The compressive strength results, especially for geopolymers based on IC, could indicate the contribution of SL to the strength of the geopolymer matrix as an increased amount of Al is introduced into the composition [34]. Large porosity and uneven pore distribution led to flexural strength reduction. For MK based geopolymers the material strength increased as porosity was reduced with a lower amount of SL. The MK precursor has higher Al content; therefore, Al coming from SL had less effect on geopolymer mechanical properties. Geopolymers based on the MK precursor had two times higher mechanical strength compared to their IC counterparts [35]. The type of filler (D or Q) had little effect on the mechanical properties of either clay precursor.

Both macrostructure and mixture composition had synergic effects on the performance of geopolymers. Greater density or closer pore structure avoids deterioration of geopolymers with lower SL content, while higher SL content gives a more durable geopolymer matrix which can withstand more extreme testing conditions.

The freeze-thaw test showed the possibility of exposing geopolymer for freezing and thawing. Geopolymers' precursors also had a significant role in freeze-thaw resistance; the test showed that material is durable and can withstand freezing and thawing for some time. The first indicator of structural changes was weight loss. Weight loss can be associated with the collapse of weaker pores and free salt dissolution in the water. Weight loss was not significant for MK based geopolymers; the strength reduction after 25 freeze-thaw cycles was from 10 to 55.3%. Higher strength loss was observed for geopolymers with low SL content, while 10 to 16.7% strength loss was seen for geopolymers with the highest SL content. Increased SL content in mixture composition negatively affected weight loss, indicating that porosity had a more critical role on structural integrity during freezing and thawing than the strength of the geopolymer matrix. Strength change results supported this. Strength reduction after 25 freeze-thaw cycles was from 13.3 to 45.0% for IC based geopolymers. Higher strength loss was observed for samples with the lowest SL content. MK-based geopolymer freeze-thaw resistance results are comparable with a new type of

cementitious materials, such as magnesium oxychloride cement foam concrete, whose strength is reduced by 12% (to 1.46 MPa) after 20 freeze-thaw cycles [36]. Cellular concrete, after 60 freeze-thaw cycles, had a strength reduction from 15 to 40% [37]. Freeze-thaw resistance was significantly improved for samples with air-voids smaller than 300 μm.

Sulfate attack on geopolymers indicated that two mass and structural change phases occurred during the test. At first, during the immersion, the sample weight can increase due to the saturation of the porous structure of geopolymer. Another scenario is associated with weight loss which may be related to a dissolution of soluble salts in the structure of geopolymers. For MK based geopolymers the trend is more predictable as the structure of the geopolymers is stronger. Only for compositions with small SL content (higher density) did the mass increase at the first stage of the test. After the first mass change, a gradual mass increase was observed as the solution may have soaked into the deeper structure of the samples, and sulfate may be attracted to the material. IC precursor geopolymer samples with high SL content showed a similar trend with initial weight loss followed by gradual weight gain.

MK based geopolymers with high SL content showed strength loss from 0.0 to 5.0%, which shows good performance of such lightweight material and confirms similar research on sulfate attack on geopolymer concrete in the literature. Previously it was reported that the main product of the geopolymerization is not affected by sulfate attack and such concrete gained strength after 90 days of soak time in magnesium sulfate solution, and no cracks or mass changes were observed [38,39].

5. Conclusions

Calcined illite and kaolin waste clay precursors combined with aluminum scrap recycling waste (salt slag) are suitable for the production of highly porous lightweight material. Such approaches reduce disposal of hazardous materials to landfills and can provide advanced material with low density and certain durability. The amount of salt slag can control the porosity, as during the activation of precursors, gas and temperature release forms the geopolymer structure. The appearance and physical properties of both precursor geopolymers are similar, but the mechanical properties and performance of the obtained materials are different. Metakaolin based geopolymers show improved mechanical performance (2.0–3.8 MPa), freeze-thaw resistance up to 50 cycles, and more predictable sulfate attack resistance with a density from 580 to 675 kg/m^3. Illite clay based geopolymer showed better performance with increased salt cake content, which indicates that salt cake participates in alkali activation with its Al contribution, resulting in a more stable geopolymer structure. During the durability tests, the poor performance of illite clay precursor was still obtained. After 25 freeze-thaw cycles, weight loss of samples was from 6.9 to 14.4. wt.%, while the strength loss was from 13.3 to 45.0%. Strength reduction after the sulfate attack test showed poor resistance and high strength loss compared to its metakaolin based geopolymer counterparts. Despite the different performance of both precursor types, it can be concluded that similar lightweight materials can be obtained from entirely waste source precursors. The application of such material proved to be suitable both in civil engineering and also in other technological processes where durability against chemical attack must be considered.

Author Contributions: Conceptualization, G.B., D.V., A.K. and D.B.; methodology, G.B., D.V., A.K. and D.B.; software, A.K. and D.B.; validation, D.V. and D.B.; formal analysis, G.B. and D.V.; investigation, G.B.; resources, D.V. and A.K.; data curation, G.B. and D.V.; writing—original draft preparation, G.B.; writing—review and editing G.B., D.V., A.K. and D.B.; visualization, G.B.; supervision, D.V., A.K. and D.B.; project administration, D.V.; funding acquisition, G.B. and D.V. All authors have read and agreed to the published version of the manuscript.

Funding: This research was funded by the European Social Fund under the No 09.3.3-LMT-K-712 "Development of Competences of Scientists, other Researchers and Students through Practical Research Activities" measure.

Institutional Review Board Statement: Not applicable.

Informed Consent Statement: Not applicable.

Data Availability Statement: Not applicable.

Conflicts of Interest: The authors declare no conflict of interest.

References

1. Alonso, S.; Palomo, A. Alkaline activation of metakaolin and calcium hydroxide mixtures: Influence of temperature, activator concentration and solids ratio. *Mater. Lett.* **2001**, *47*, 55–62. [CrossRef]
2. Williams, I.; Riessen, A. Van thermal barriers. *Appl. Clay Sci.* **2009**, *46*, 6–11. [CrossRef]
3. Temuujin, J.; van Riessen, A.; Williams, R. Influence of calcium compounds on the mechanical properties of fly ash geopolymer pastes. *J. Hazard. Mater.* **2009**, *167*, 82–88. [CrossRef]
4. Habert, G.; d'Espinose de Lacaillerie, J.B.; Roussel, N. An environmental evaluation of geopolymer based concrete production: Reviewing current research trends. *J. Clean. Prod.* **2011**, *19*, 1229–1238. [CrossRef]
5. Zain, H.; Abdullah, M.M.A.B.; Hussin, K.; Ariffin, N.; Bayuaji, R. Review on Various Types of Geopolymer Materials with the Environmental Impact Assessment. In *MATEC Web of Conferences*; EDP Sciences: Les Ulis, France, 2017; Volume 97.
6. Sgarlata, C.; Formia, A.; Siligardi, C.; Ferrari, F.; Leonelli, C. Mine Clay Washing Residues as a Source for Alkali-Activated Binders. *Materials* **2021**, *15*, 83. [CrossRef]
7. Boca Santa, R.A.A.; Soares, C.; Riella, H.G. Geopolymers with a high percentage of bottom ash for solidification/immobilization of different toxic metals. *J. Hazard. Mater.* **2016**, *318*, 145–153. [CrossRef]
8. Deevasan, K.K.; Ranganath, R.V. Geopolymer concrete using industrial byproducts. *Proc. ICE-Constr. Mater.* **2011**, *164*, 43–50. [CrossRef]
9. Komnitsas, K.; Zaharaki, D.; Vlachou, A.; Bartzas, G.; Galetakis, M. Effect of synthesis parameters on the quality of construction and demolition wastes (CDW) geopolymers. *Adv. Powder Technol.* **2015**, *26*, 368–376. [CrossRef]
10. Vaičiukynienė, D.; Tamošaitis, G.; Kantautas, A.; Nizevičienė, D.; Pupeikis, D. Porous alkali-activated materials based on municipal solid waste incineration ash with addition of phosphogypsum powder. *Constr. Build. Mater.* **2021**, *301*, 123962. [CrossRef]
11. Shen, J.; Li, Y.; Lin, H.; Lv, J.; Feng, S.; Ci, J. Early properties and microstructure evolution of alkali-activated brick powder geopolymers at varied curing humidity. *J. Build. Eng.* **2022**, *54*, 104674. [CrossRef]
12. Borg, R.P.; Vaičiukynienė, D.; Gurskis, V.; Nizevičienė, D.; Skominas, R.; Ramukevičius, D.; Sadzevičius, R. Alkali-Activated Material Based on Red Clay and Silica Gel Waste. *Waste Biomass Valorization* **2020**, *11*, 2973–2982. [CrossRef]
13. Ghadir, P.; Ranjbar, N. Clayey soil stabilization using geopolymer and Portland cement. *Constr. Build. Mater.* **2018**, *188*, 361–371. [CrossRef]
14. Samantasinghar, S.; Singh, S.P. Strength and Durability of Granular Soil Stabilized with FA-GGBS Geopolymer. *J. Mater. Civ. Eng.* **2021**, *33*, 06021003. [CrossRef]
15. Min, Y.; Wu, J.; Li, B.; Zhang, M.; Zhang, J. Experimental study of freeze–thaw resistance of a one-part geopolymer paste. *Case Stud. Constr. Mater.* **2022**, *17*, e01269. [CrossRef]
16. Tan, J.; Dan, H.; Ma, Z. Metakaolin based geopolymer mortar as concrete repairs: Bond strength and degradation when subjected to aggressive environments. *Ceram. Int.* **2022**, *48*, 23559–23570. [CrossRef]
17. Zhang, J.; Shi, C.; Zhang, Z.; Hu, X. Reaction mechanism of sulfate attack on alkali-activated slag/fly ash cements. *Constr. Build. Mater.* **2022**, *318*, 126052. [CrossRef]
18. Yang, T.; Gao, X.; Zhang, J.; Zhuang, X.; Wang, H.; Zhang, Z. Sulphate resistance of one-part geopolymer synthesized by calcium carbide residue-sodium carbonate-activation of slag. *Compos. Part B Eng.* **2022**, *242*, 110024. [CrossRef]
19. Padamata, S.K.; Yasinskiy, A.; Polyakov, P. A Review of Secondary Aluminum Production and Its Byproducts. *JOM* **2021**, *73*, 2603–2614. [CrossRef]
20. Jafari, N.H.; Stark, T.D.; Roper, R. Classification and Reactivity of Secondary Aluminum Production Waste. *J. Hazard. Toxic Radioact. Waste* **2014**, *18*, 04014018. [CrossRef]
21. Shinzato, M.C.; Hypolito, R. Solid waste from aluminum recycling process: Characterization and reuse of its economically valuable constituents. *Waste Manag.* **2005**, *25*, 37–46. [CrossRef]
22. Calder, G.V.; Stark, T.D. Aluminum Reactions and Problems in Municipal Solid Waste Landfills. *Pract. Period. Hazard. Toxic Radioact. Waste Manag.* **2010**, *14*, 258–265. [CrossRef]
23. Rugele, K.; Bumanis, G.; Mezule, L.; Juhna, T.; Bajare, D. Application of industrial wastes in renewable energy production. *Agron. Res.* **2015**, *13*, 526–532.
24. Gruskevica, K.; Bumanis, G.; Tihomirova, K.; Bajare, D.; Juhna, T. Alkaline activated material as the adsorbent for uptake of high concentration of zinc from wastewater. In *Key Engineering Materials*; Trans Tech Publications Ltd.: Wollerau, Switzerland, 2017; Volume 721 KEM, ISBN 9783035710724.
25. Novais, R.M.; Buruberri, L.H.H.; Seabra, M.P.P.; Labrincha, J.A.A. Novel porous fly-ash containing geopolymer monoliths for lead adsorption from wastewaters. *J. Hazard. Mater.* **2016**, *318*, 631–640. [CrossRef]

26. Bumanis, G.; Novais, R.M.; Carvalheiras, J.; Bajare, D.; Labrincha, J.A. Metals removal from aqueous solutions by tailored porous waste-based granulated alkali-activated materials. *Appl. Clay Sci.* **2019**, *179*, 105147. [CrossRef]
27. Strozi, M.; Raymundo, M.; Colombo, P. Effect of process parameters on the physical properties of porous geopolymers obtained by gelcasting. *Ceram. Int.* **2014**, *40*, 13585–13590. [CrossRef]
28. Bajare, D.; Korjakins, A.; Kazjonovs, J.; Rozenstrauha, I. Pore structure of lightweight clay aggregate incorporate with non-metallic products coming from aluminium scrap recycling industry. *J. Eur. Ceram. Soc.* **2012**, *32*, 141–148. [CrossRef]
29. Bajare, D.; Korjakins, A.; Kazjonovs, J. Application of Aluminium Dross and Glass Waste for Production of Expanded Clay Aggregate. *Civ. Eng.* **2011**, *11*, 27–31.
30. *LVS 156-1:2009*; Concrete—National Annex of Latvian Standard to European Standard EN 206-1—Part 1: Requirements for Classification and Attestation of Conformity. LVS/STK/04: Rīga, Latvia, 2009.
31. Ercoli, R.; Laskowska, D.; Nguyen, V.V.; Le, V.S.; Louda, P.; Ło´s, P.Ł.; Ciemnicka, J.; Prałat, K.; Renzulli, A.; Paris, E.; et al. Mechanical and Thermal Properties of Geopolymer Foams (GFs) Doped with By-Products of the Secondary Aluminum Industry. *Polymers* **2022**, *14*, 703. [CrossRef]
32. Bumanis, G. Alkali Activated Materials and Its Applications. Ph.D. Thesis, Riga Technical University, Riga, Latvia, 2015.
33. Hall, C.; Hamilton, A. Porosity–density relations in stone and brick materials. *Mater. Struct. Constr.* **2015**, *48*, 1265–1271. [CrossRef]
34. López, F.J.; Sugita, S.; Tagaya, M.; Kobayashi, T. Metakaolin-Based Geopolymers for Targeted Adsorbents to Heavy Metal Ion Separation. *J. Mater. Sci. Chem. Eng.* **2014**, *2*, 16–27. [CrossRef]
35. Swanepoel, J.C.; Strydom, C. Utilisation of fly ash in a geopolymeric material. *Appl. Geochem.* **2002**, *17*, 1143–1148. [CrossRef]
36. Zhong, D.; Wang, S.; Gao, Y.; Wang, L.; Feng, K. Experimental study on freeze-thaw resistance of modified magnesium oxychloride cement foam concrete. *J. Phys. Conf. Ser.* **2021**, *1885*, 32009. [CrossRef]
37. Shon, C.S.; Lee, D.; Kim, J.H.; Chung, C.W. Freezing and thawing resistance of cellular concrete containing binary and ternary cementitious mixtures. *Constr. Build. Mater.* **2018**, *168*, 73–81. [CrossRef]
38. Ghanem, G.; Yehia, S.; Mohamed, N.; Helmy, M. Effect of Sulphate Attack on Compressive Strength of Geopolymer Concrete. *Int. J. Sci. Eng. Res.* **2022**, *13*, 63–70.
39. Alyousef, R.; Ebid, A.A.K.; Huseien, G.F.; Mohammadhosseini, H.; Alabduljabbar, H.; Ngian, S.P.; Mohamed, A.M. Effects of Sulfate and Sulfuric Acid on Efficiency of Geopolymers as Concrete Repair Materials. *Gels* **2022**, *8*, 53. [CrossRef]